Nitrogen K-shell photoelectron angular distribution from NO molecules in the molecular frame

2008 J. Phys. B: At. Mol. Opt. Phys. 41 045102

(http://iopscience.iop.org/0953-4075/41/4/045102)

J. Phys. B: At. Mol. Opt. Phys. **41** (2008) 045102 (6pp) doi:10.1088/0953-4075/41/4/045102

Nitrogen K-shell photoelectron angular distribution from NO molecules in the molecular frame

H Fukuzawa[1], X-J Liu[1], R Montuoro[2], R R Lucchese[1], Y Morishita[3], N Saito[3], M Kato[3], I H Suzuki[3], Y Tamenori[4], T Teranishi[1], T Lischke[1], G Prümper[1] and K Ueda[1]

[1] Institute of Multidisciplinary Research for Advanced Materials, Tohoku University, Sendai 980-8577, Japan
[2] Department of Chemistry, Texas A&M University, College Station, TX 77843-3255, USA
[3] National Metrology Institute of Japan, AIST, Tsukuba 305-8568, Japan
[4] Japan Synchrotron Radiation Research Institute, Sayo-gun, Hyogo 679-5198, Japan

E-mail: lucchese@mail.chem.tamu.edu and ueda@tagen.tohoku.ac.jp

Received 12 December 2007, in final form 16 January 2008
Published 12 February 2008
Online at stacks.iop.org/JPhysB/41/045102

Abstract
Molecular-frame photoelectron angular distributions (MFPADs) for NO in the nitrogen K-shell ionization regions have been measured at five photon energies 412, 413, 413.22, 414.5 and 415 eV. All experimental information on the MFPAD is encapsulated in a set of four $F_{JN}(\theta)$ functions for each energy, which are compared with the results of full *ab initio* vibrationally averaged calculations, performed using the multichannel Schwinger configuration interaction method within the framework of the adiabatic approximation for photoionization. The major features are fairly well reproduced by the calculations.

(Some figures in this article are in colour only in the electronic version)

1. Introduction

Molecular photoionization is one of the simplest reactions, yet it has been receiving continuous and remarkable attention as it provides a wealth of information about the target molecule. With the advent of new-generation synchrotron sources and multiple coincidence techniques, studies of the photoionization of free molecules are rapidly developing. From a theoretical perspective, the most straightforward description of a molecular photoionization process may be obtained in the molecular frame. One established experimental approach to the study of photoionization in the molecular frame is to make angle-resolved photoelectron–photoion coincidence measurements in the case of dissociative photoionization processes [1, 2]. A remarkable breakthrough in the experimental investigation of molecular-frame photoelectron angular distributions (MFPADs) has been brought by the use of position-sensitive detectors [3–8]. To date, these techniques have been extensively used to study the MFPADs of the diatomic and linear polyatomic molecules (see, for example, [9–17]). The MFPADs of K-shell photoelectrons from small molecules have been particularly insightful in the region of shape resonances, where they provide a window on the underlying partial-wave composition of the wavefunction describing the outgoing photoelectron travelling within the anisotropic potential of the ion [2].

In the present work, we have investigated experimentally and theoretically N 1s MFPADs of nitric oxide. The electronic configuration of the NO molecule in the X $^2\Pi$ ground state is

$$1\sigma^2 2\sigma^2 3\sigma^2 4\sigma^2 1\pi^4 5\sigma^2 2\pi^1,$$

where 1σ and 2σ are, to a good approximation, the O 1s and N 1s atomic core orbitals. Photoionization of the N 1s orbital in NO may produce ions in two different electronic states, $2\sigma 2\pi\ ^3\Pi$ and $^1\Pi$, separated in energy by 1.5 eV by the exchange interaction between the 2σ and 2π orbitals [18]. The ionization thresholds have been determined to be 410.34 eV for the $^3\Pi$ state and 411.81 eV for $^1\Pi$ [19].

Two broad maxima appear at about 413 and 415 eV in the N 1s absorption and electron-energy loss spectrum

[19–21], and the assignment of these structures is under debate. The current status of the matter has been well summarized by Hosaka *et al* [22], who attributed the first peak at 413 eV to doubly excited states while the peak at 415 eV to a shape resonance, on the basis of multiplet-resolved photoionization partial cross section measurements. On the other hand, Lin and Lucchese suggested that the maxima may be mainly the result of both $^3\Pi$ and $^1\Pi$ coupled photoionization channels [23]. Hosaka *et al* also reported the MFPADs of N 1s photoemission from NO for the molecular axis parallel to the electric vector of the light [24].

In the present paper, we report measured and calculated MFPADs for N 1s photoemission from NO at photon energies between 412 and 415 eV, i.e. in the energy region across the two maxima. Theoretical results are obtained in a complete *ab initio* approach, where the photoionization amplitudes computed by the multichannel Schwinger configuration interaction (MCSCI) method are averaged vibrationally using the eigenfunctions of model vibrational Hamiltonians, built on the basis of energy profiles computed at the configuration interaction (CI) level for the molecular ground state and at the complete active space self-consistent field (CASSCF) level for each of the electronic states of the parent ion. In the experiment, we employ coincidence momentum imaging spectroscopy, in which coincidence signals between the N 1s photoelectron and the ion pair N^+–O^+ are selected.

2. Experiment

The experiment was performed on the c branch of the soft x-ray photochemistry beam line 27SU [25–27] at SPring-8. The storage ring was operated in the 73 single bunches + 10/84 filling mode, which provides a single-bunch separation of 57.0 ns. The coincidence measurements described below were made with the electric vector (polarization vector) E orientated vertically. The photon beam was focused on a spot of size less than 0.2 mm in height and 0.5 mm in width at the intersection with the molecular beam. The present electron-ion multiple coincidence momentum imaging technique is based on recording the time of flight (TOF) of both electrons and ions by multi-hit two-dimensional position-sensitive detectors [7, 15, 28]. The two TOF spectrometers are placed face to face, and their axes are horizontal and perpendicular to both the photon beam and the molecular beam. The acceleration region and the drift region of the electron spectrometer have lengths of 33.7 mm and 67.4 mm, respectively. The electron spectrometer is equipped with a hexagonal multi-hit position-sensitive delay-line detector of 120 mm effective diameter (Roentdek HEX120). For the ion spectrometer, there are two acceleration regions and no drift region. The length of the first acceleration region is 11.5 mm and that of the second one is 89.0 mm. The ion spectrometer is equipped with a similar delay-line detector of 80 mm effective diameter (Roentdek HEX80). The TOFs of the electrons and ions were recorded with respect to the bunch marker of the synchrotron radiation source using multi-hit time-to-digital converters (TDCs). These TDCs have a timing resolution of about 120 ps, a multi-hit capability of up to 6 events and a time span of 40 μs [29]. Appropriate gates select only those electron signals synchronized with the single bunches, and we record only events in which at least one ion (or two ions) and one electron are detected in coincidence. Knowledge of position and arrival time on the particle detectors, (x, y, t), allows us to extract information about the linear momentum (p_x, p_y, p_z) for each particle. N 1s MFPADs were measured using electron-ion-ion coincidence mode at photon energies of 412, 413, 413.22, 414.5 and 415 eV. The N $1s^{-1}$ $^3\Pi$ ionization threshold energy is 410.34 eV [19]. The photon energy bandwidth was 80 meV. The NO molecular beam was produced at a stagnation pressure of 1.0 bar through a pinhole of 30 μm diameter and 0.25 mm thickness. The static extraction field was set to 0.5 V mm^{-1} at photon energies of 412–414.5 eV and 0.7 V mm^{-1} at a photon energy of 415 eV. The static field of the second acceleration region for the ions was set to 26 V mm^{-1}. A uniform magnetic field of 1.5, 2 and 3 G was imposed on the spectrometer at photon energies of 412, 413–414.5 and 415 eV, respectively, by a set of Helmholtz coils outside the vacuum chamber.

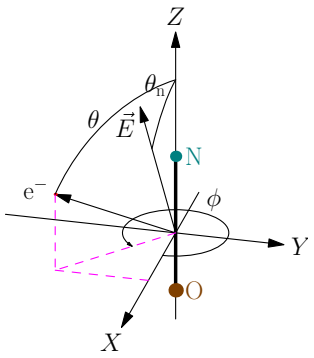

Figure 1. Molecular frame. Note that for the case of linear molecules considered here, we have taken the X axis to lie in the plane defined by the Z and E axes.

3. Theory

3.1. The MFPAD in the dipole approximation

Linearly polarized light may be fully characterized by a single vector, e.g. the electric vector E, as shown in figure 1. Thus, for linear molecules, the MFPADs will depend on three angles, θ and ϕ, which give the direction of emission of the photoelectron in the molecular frame, and θ_n, which is the polar angle describing the orientation of the molecular axis with respect to the direction of polarization. Note that for arbitrary molecular systems, an additional azimuthal angle would have been employed to describe the orientation of the E axis in the molecular frame. However, for linear systems, the value of such an azimuthal angle becomes arbitrary and we will set it to zero by locating the X axis in the plane defined by the Z and E axes as indicated in figure 1.

The angular dependence of the MFPAD may be analysed by projecting the intensity $I(\theta, \phi, \theta_n)$ on a basis set built as the direct product of a complete set of spherical harmonics for

each of the directions of the photoelectron and the molecule. In the case of linear molecules, we obtain

$$I(\theta, \phi, \theta_n) = \sum_{J'JN} H_{J'JN} Y_{J'N}(\theta, \phi) Y^*_{JN}(\theta_n, 0). \quad (1)$$

Within the dipole approximation, the photoionization process is described by the transition matrix elements

$$I_{lm\mu} = \left\langle \Psi^i | d_\mu | \sum_\beta \Phi^f_\beta \psi^{(-)}_{\beta,\alpha lm} \right\rangle, \quad (2)$$

coupling the initial state Ψ^i by the spherical component μ of the dipole operator d_μ to the coupled-channel ionized state which is written as a sum of appropriately antisymmetrized products of the ion states Φ^f_β and photoelectron wavefunctions $\psi^{(-)}_{\beta,\alpha lm}$. In equation (2), the subscript (αlm) and superscript $(-)$ indicate that the asymptotic form of the wavefunction has the photoelecton leaving the molecule in partial wave (lm) with the ion in state Φ^f_α. This leads to the following expression for the expansion coefficients $H_{J'JN}$:

$$H_{J'JN} = \frac{4\pi^2 E}{c} \sum_{\substack{lm\mu \\ l'm'\mu'}} (-1)^{m+\mu'} \left[\frac{(2l+1)(2l'+1)}{(2J+1)(2J'+1)} \right]^{\frac{1}{2}} \times I_{lm\mu} I^*_{l'm'\mu'} \langle ll'00|J'0\rangle \langle l, l', -m, m'|J'N\rangle \times \langle 1100|J0\rangle \langle 1, 1, \mu, -\mu'|J, N\rangle, \quad (3)$$

where E is the photon energy, c is the speed of light and $\langle l, l', m, m'|JN\rangle$ is a Clebsch–Gordan coefficient.

The dependence of the intensity on ϕ and θ_n in equation (1) may be treated explicitly. In the case of linearly polarized light, the MFPAD may be written as [29]

$$I(\theta, \phi, \theta_n) = F_{00}(\theta) + F_{20}(\theta) P^0_2(\cos\theta_n) + F_{21}(\theta) P^1_2(\cos\theta_n) \cos\phi + F_{22}(\theta) P^2_2(\cos\theta_n) \cos 2\phi. \quad (4)$$

The F_{JN} functions can be expanded in Legendre polynomials as

$$F_{JN}(\theta) = \sum_{J'} C_{J'JN} P^N_{J'}(\cos\theta), \quad (5)$$

where the $C_{J'JN}$ expansion coefficients may be written in terms of the $H_{J'JN}$ coefficients as

$$C_{J'JN} = \frac{1}{2\pi(1+\delta_{N,0})} \times \left[\frac{(2J'+1)(2J+1)(J'-N)!(J-N)!}{(J'+N)!(J+N)!} \right]^{\frac{1}{2}} H_{J'JN}. \quad (6)$$

All possible experimental information is then encapsulated in the four $F_{JN}(\theta)$ functions.

When vibrationally resolved experiments are considered, equation (1) may be applied to every single vibrationally specific intensity measured. Therefore we may obtain a new set of vibrationally specific coefficients $\mathcal{H}^{\nu\nu^+}_{J'JN}$ that will lead to vibrationally specific $\mathcal{F}^{\nu\nu^+}_{JN}(\theta)$ functions through equations (5) and (6), where ν and ν^+ are the vibrational quantum numbers for the initial and the ion states, respectively. The vibrationally specific coefficients $\mathcal{H}^{\nu\nu^+}_{J'JN}$ are in turn obtained from the vibrationally resolved photoionization matrix elements $\mathcal{I}^{\nu\nu^+}_{lm\mu}$—explicitly including the transition between specific vibrationally excited states—by the analogue of equation (3). The meaning of such transition matrix elements will be discussed in detail elsewhere [30].

Note that we can easily obtain vibrationally unresolved $F_{JN}(\theta)$ functions for ionization from the ground vibrational state ($\nu = 0$) by summing over the vibrational states of the ion:

$$F_{JN}(\theta) = \sum_{\nu^+} \mathcal{F}^{0\nu^+}_{JN}(\theta). \quad (7)$$

If more than one initial vibrational state is occupied, then an appropriate average over initial state populations must also be performed. The same relation between vibrationally resolved and unresolved coefficients obviously holds for $H_{J'JN}$ and $C_{J'JN}$ as well.

3.2. *Ab initio* calculations

Theoretical vibrationally averaged F_{JN} functions were obtained using equation (7). The required vibrationally specific transition amplitudes $\mathcal{I}^{\nu\nu^+}_{lm\mu}$ have been computed as described thoroughly in our study of vibrationally resolved cross sections and asymmetry parameter for NO N 1s photoionization [30]. Thus, we will limit the following description to a brief outline.

The theoretical method employed has been established by some of the present authors [31], and it is based on the approximation that the dipole matrix elements of photoionization $I_{lm\mu}$ change adiabatically with distortions in the nuclear geometry due to the vibrational motion. This allows us to obtain transition matrix elements for specific initial (ν) and final (ν^+) vibrational states $\mathcal{I}^{\nu\nu^+}_{lm\mu}$ by averaging $I_{lm\mu}$ over the vibrational coordinates involved with the product of the corresponding vibrational wavefunctions. In a fully *ab initio* framework, these vibrational wavefunctions are obtained by diagonalizing model vibrational Hamiltonians built for each electronic states using the electronic energy profiles computed at the multireference restricted CI level for the X $^2\Pi$ state of NO, and by complete active space self-consistent field (CASSCF) calculations for the N $1s^{-1}$ $^3\Pi$ and $^1\Pi$ ionic states. The six σ orbitals included in the target states include the two 1s core orbitals and one virtual σ orbital, and the two π orbitals (1π and 2π, including both $m = +1$ and $m = -1$ components) were the two occupied π orbitals. Then both in the CASSCF calculation used to obtain the orbitals and the CI calculations for the initial and ionized states, complete CI calculations were performed with this orbital space (six σ and two π) and with all electrons active. In all the calculations of the electronic states, the active space included six σ and two π orbitals optimized for the ground state of the ion NO^+. We obtained the values of 242 meV, 241 meV and 235 meV for the vibrational frequencies of NO X $^2\Pi$, NO^+ N $1s^{-1}$ $^3\Pi$ and $^1\Pi$ states, which are respectively comparable to the experimental estimates of 236.0 meV, 204.7 meV and 228.9 meV [30].

In order to compute the average of the dipole matrix elements, we derived analytical expressions by fitting the values of each $I_{lm\mu}$—obtained by fixed-nuclei multichannel

Schwinger configuration interaction (MCSCI) calculations—to fourth-degree/first-degree complex rational functions, supplemented by a fifth-degree polynomial to improve accuracy in some cases. Converged results were obtained using a grid of ten evenly distributed values of NO bond length ranging from −0.15 Å to +0.15 Å around the experimental value of 1.15077 Å for the NO equilibrium distance [32]. Assuming that only the ground vibrational state is populated in the neutral molecule ($\nu = 0$) and including the $\nu' = 0, 1, 2$ states in the parent ion, we were able to account for the 99.98% of the photoionization intensity.

The electronic wavefunctions were computed using the augmented triple-ζ (aug-cc-pVTZ) basis set of Dunning and co-workers [33, 34]. The final state included only the two main N $1s^{-1}$ photoionization channels, NO^+ $^3\Pi$,$^1\Pi$. The Schwinger dipole matrix elements $I_{lm\mu}$ were computed using a single-centre basis set including functions with ℓ up to 120 for bound and continuum orbitals, reduced to $\ell \leqslant 18$ in the photoelectron asymptotic region. At the equilibrium geometry of NO we found the vertical ionization potentials to be 411.69 eV for the N $1s^{-1}$ $^3\Pi$ state and 412.54 eV for the N $1s^{-1}$ $^1\Pi$ state, slightly above the experimental values of 410.34 eV and 411.81 eV [19].

4. Results and discussion

There are a number of possible approaches for obtaining F_{JN}^{MFPAD} or equivalently the electron-frame photoelectron angular distribution (EFPAD) [35] F_{JN}^{EFPAD} functions from angle-resolved photoelectron–photoion coincidence measurements. If the full 4π angular distributions of the photoelectron and ion recoil directions have been measured, then it is possible to use the projection methods [35, 36]. The projection methods rely on the fact that the expansions in equation (4) are in terms of orthogonal polynomials of θ_{n} and ϕ such that $F_{JN}(\theta)$ can be obtained as

$$F_{JN}(\theta) = \frac{(2J+1)(J-N)!}{2\pi(1+\delta_{N,0})(J+N)!} \times \int_0^{\pi} \sin\theta_{\mathrm{n}}\,\mathrm{d}\theta_{\mathrm{n}} \int_0^{2\pi} \mathrm{d}\phi\, I(\theta,\phi,\theta_{\mathrm{n}})\, P_J^N(\cos\theta_{\mathrm{n}})\cos(N\phi). \tag{8}$$

The experimental cross sections are relative and thus the F_{JN} functions are normalized to dimensionless $\bar{F}_{JN}$ functions, where

$$\int_0^{\pi} \sin\theta\,\mathrm{d}\theta \int_0^{2\pi} \mathrm{d}\phi\, \bar{F}_{00}(\theta) = 4\pi. \tag{9}$$

In figures 2 and 3, we present the experimental $\bar{F}_{JN}$ functions determined for N $1s^{-1}$ $^3\Pi$ and $^1\Pi$ states, respectively, of NO^+, using the projection methods given in equation (8) for five different photon energies. The $\theta = 0^\circ$ direction corresponds to the direction that the N^+ atom was emitted and $\theta = 180^\circ$ corresponds to the direction of emission of the O^+ atom.

Using the obtained $\bar{F}_{JN}$ functions, we can reconstruct the MFPADs for any set of angles between the molecular axis and the polarization vector. The reconstructed MFPADs for

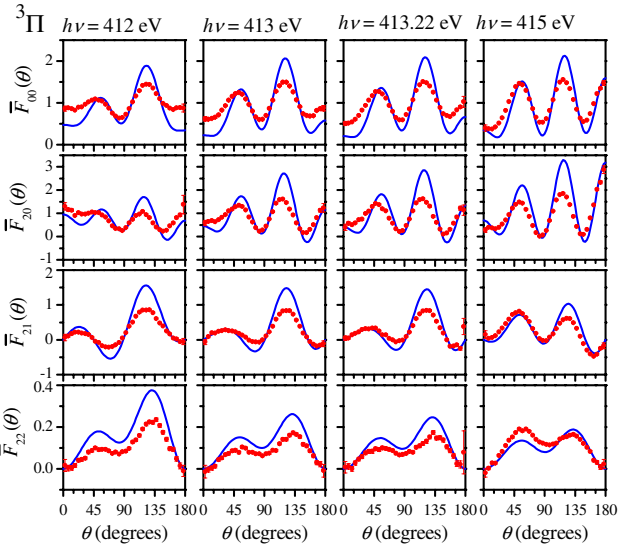

Figure 2. A comparison between the measured (dots) and calculated (lines) F_{JN} functions for photoionization of NO leading to the N $1s^{-1}$ $^3\Pi$ state of NO^+ at photon energies of 412, 413, 413.22 and 415 eV.

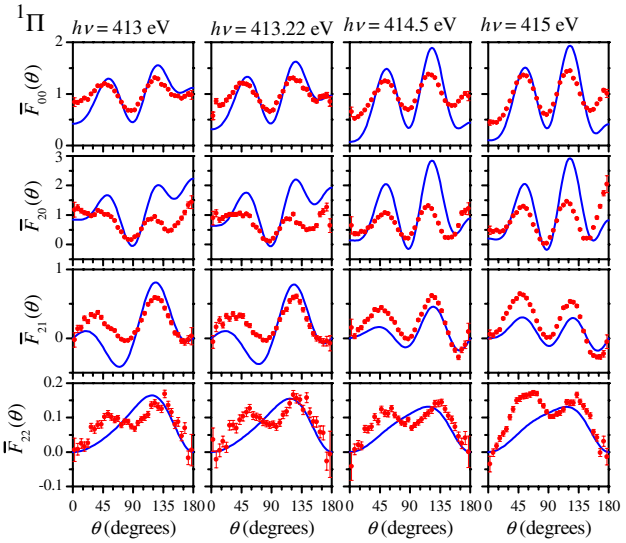

Figure 3. A comparison between the measured (dots) and calculated (lines) F_{JN} functions for photoionization of NO leading to the N $1s^{-1}$ $^1\Pi$ state of NO^+ at photon energies of 413, 413.22, 414.5 and 415 eV.

the angles of the polarization vector of 0°, 45° and 90° with respect to the molecular axis are illustrated in figures 4 and 5 for NO^+ N 1 s^{-1} $^3\Pi$ and $^1\Pi$ states, respectively. The electron emission is within the plane defined by the molecular axis and the electric vector of the incident radiation. Hosaka *et al* [24] measured the MFPADs at photon energies of 413.5, 415, 417 and 421 eV. They provided the MFPADs only for the case that the molecular axis is parallel (0°) to the polarization vector. The structure of our MFPAD for 0° in figures 4 and 5 is in general close to that of their MFPAD at a similar energy.

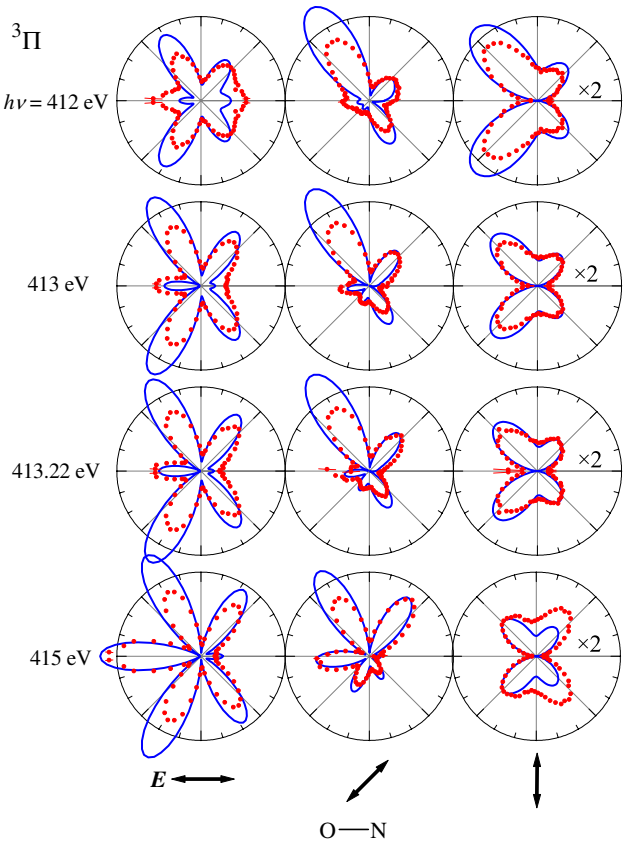

Figure 4. A comparison between the measured (dots) and calculated (lines) MFPADs for photoionization of NO leading to the N $1s^{-1}\,^3\Pi$ state of NO^+, on the plane with the molecular axis and E vector, at photon energies of 412, 413, 413.22 and 415 eV. The molecular axis is horizontal and the E vector is 0°, 45° and 90° with respect to the molecular axis.

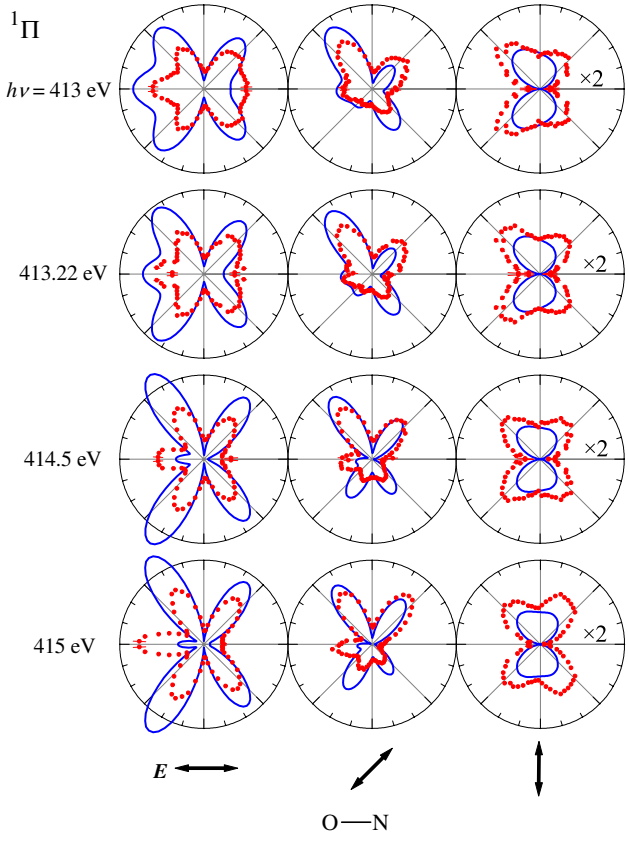

Figure 5. A comparison between the measured (dots) and calculated (lines) MFPADs for photoionization of NO leading to the N $1s^{-1}\,^1\Pi$ state of NO^+, on the plane with the molecular axis and E vector, at photon energies of 413, 413.22, 414.5 and 415 eV. The molecular axis is horizontal and the E vector is 0°, 45° and 90° with respect to the molecular axis.

In figures 2–5, we also present the results of the *ab initio* calculations. The same normalization is applied to the theoretical F_{JN} functions given in figures 2 and 3. The observed major features are fairly well reproduced by the calculations. In the MFPADs of figures 4 and 5, as was seen in the earlier study [24], we note a strong f wave appearance of the MFPADs in the case of polarization parallel to the molecular axis for photon energies of ∼415 eV, both for NO^+ N 1 $s^{-1}\,^3\Pi$ and $^1\Pi$ states. We find that the shape resonance peaks appear at ∼415 eV and ∼414.5 eV for NO^+ N $1s^{-1}\,^3\Pi$ and $^1\Pi$ states, respectively, in the vibrationally summed partial cross sections of the present *ab initio* calculations: these two peaks form a single peak in the total ionization cross section [30]. Thus, the strong f wave appearance of the MFPADs at ∼415 eV can indeed be attributed to the σ^* shape resonance.

The most significant qualitative difference between theory and experiment is in the $\bar{F}_{22}$ functions for the $^1\Pi$ state shown in figure 3. In this case, the experiments show two pronounced peaks at about 45° and 135° with the theory having only one peak at ∼120°. Restriction of the present calculations to the two main photoionization channels, N $1s^{-1}\,^3\Pi$ and $^1\Pi$, might be the cause of some of the discrepancies observed in figures 2–5. The discrepancy in the features seen in experimental and theoretical MFPADs of figures 4 and 5 at low energies of 412 to 413.22 eV may be caused by resonances due to autoionizing states, which can be expected to occur below the thresholds of shake-up states that should be present above the N 1s thresholds. No such states have been included into the present calculations.

5. Conclusion

Employing coincidence momentum imaging spectroscopy, we have measured molecular-frame photoelectron angular distributions (MFPAD) for NO in the nitrogen K-shell ionization regions at five photon energies 412, 413, 413.22, 414.5 and 415 eV. Using the projection methods, we have encapsulated all experimental information of the MFPAD at each energy in the four $F_{JN}(\theta)$ functions. We have also performed full *ab initio* vibrationally averaged calculations for the MFPADs using the multichannel Schwinger configuration interaction (MCSCI) method within Chase's adiabatic approximation. The agreement between the results of present calculations and the measurements is fairly good. The present observation of the strong f wave appearance of the MFPADs at ∼415 eV is consistent with the assignment of the σ^* shape

resonances at ∼415 eV. To confirm the origin for the first peak at ∼413 eV observed in the absorption spectrum, one needs to extend the *ab initio* calculations to include the multi-electron excitation states. Also, the measurements for the vibrationally resolved MFPADs will be insightful. Such theoretical and experimental studies are in progress.

Acknowledgments

The measurements were carried out with the approval of JASRI and supported in part by Grants-in-Aid for Scientific Research from the Japan Society for the Promotion of Science (JSPS). The authors are grateful to the staff of SPring-8 for their help in the course of these studies. XJL, RRL and TL gratefully acknowledge JSPS for financial support and the hospitality of the Tohoku University. RRL also acknowledges the support of the Robert A Welch Foundation (Houston, Texas) under grant A-1020.

References

[1] Golovin A V, Kuznetsov V V and Cherepkov N A 1990 *Sov. Tech. Phys. Lett.* **16** 363
[2] Shigemasa E, Adachi J, Oura M and Yagishita A 1995 *Phys. Rev. Lett.* **74** 359
[3] Heiser F, Gessner O, Viefhaus J, Wieliczek K, Hentges R and Becker U 1997 *Phys. Rev. Lett.* **79** 2435
[4] Lafosse A, Lebech M, Brenot J C, Guyon P M, Jagutzki O, Spielberger L, Vervloet M, Houver J C and Dowek D 2000 *Phys. Rev. Lett.* **84** 5987
[5] Takahashi M, Cave J P and Eland J H D 2000 *Rev. Sci. Instrum.* **71** 1337
[6] Landers A *et al* 2001 *Phys. Rev. Lett.* **87** 013002
[7] Saito N *et al* 2003 *J. Phys. B: At. Mol. Opt. Phys.* **36** L25
[8] Hosaka K, Adachi J, Golovin A V, Takahashi M, Watanabe N and Yagishita A 2006 *Japan. J. Appl. Phys.* **45** 1841
[9] Weber T *et al* 2001 *J. Phys. B: At. Mol. Opt. Phys.* **34** 3669
[10] Lafosse A, Brenot J C, Guyon P M, Houver J C, Golovin A V, Lebech M, Dowek D, Lin P and Lucchese R R 2002 *J. Chem. Phys.* **117** 8368
[11] Jahnke T *et al* 2002 *Phys. Rev. Lett.* **88** 073002
[12] Osipov T, Cocke C L, Prior M H, Landers A, Weber T, Jagutzki O, Schmidt L, Schmidt-Böcking H and Dörner R 2003 *Phys. Rev. Lett.* **90** 233002
[13] Jahnke T *et al* 2004 *Phys. Rev. Lett.* **93** 083002
[14] Lebech M, Houver J C, Dowek D and Lucchese R R 2004 *J. Chem. Phys.* **120** 8226
[15] Saito N *et al* 2005 *J. Phys. B: At. Mol. Opt. Phys.* **38** L277
[16] Li W B, Montuoro R, Houver J C, Journel L, Haouas A, Simon M, Lucchese R R and Dowek D 2007 *Phys. Rev.* A **75** 052718
[17] Teramoto T, Adachi J, Yamazaki M, Yamanouchi K, Stener M, Decleva P and Yagishita A 2007 *J. Phys. B: At. Mol. Opt. Phys.* **40** 4033
[18] Siegbahn K *et al* 1969 *ESCA Applied to Free Molecules* (Amsterdam: North-Holland)
[19] Remmers G, Domke M, Puschmann A, Mandel T, Kaindl G, Hudson E and Shirley D A 1993 *Chem. Phys. Lett.* **214** 241
[20] Wight G R and Brion C E 1974 *J. Electron. Spectrosc. Relat. Phenom.* **4** 313
[21] Kosugi N, Adachi J, Shigemasa E and Yagishita A 1992 *J. Chem. Phys.* **97** 8842
[22] Hosaka K, Adachi J, Takahashi M and Yagishita A 2003 *J. Phys. B: At. Mol. Opt. Phys.* **36** 4617
[23] Lin P and Lucchese R R 2001 *J. Synchrotron Radiat.* **8** 150
[24] Hosaka K, Adachi J, Takahashi M, Yagishita A, Lin P and Lucchese R R 2004 *J. Phys. B: At. Mol. Opt. Phys.* **37** L49
[25] Ohashi H, Ishiguro E, Tamenori Y, Kishimoto H, Tanaka M, Irie M, Tanaka T and Ishikawa T 2001 *Nucl. Instrum. Methods* A **467–468** 529
[26] Ohashi H *et al* 2001 *Nucl. Instrum. Methods* A **467–468** 533
[27] Ueda K 2003 *J. Phys. B: At. Mol. Opt. Phys.* **36** R1
[28] Ueda K and Eland J H D 2005 *J. Phys. B: At. Mol. Opt. Phys.* **38** S839
[29] Morishita Y *et al* 2005 *J. Electron. Spectrosc. Relat. Phenom.* **144–147** 255
[30] Hoshino M, Montuoro R, Lucchese R R, De Fanis A, Hergenhahn U, Tanaka T, Tanaka H and Ueda K 2008 *J. Phys. B: At. Mol. Opt. Phys.* submitted
[31] Montuoro R, Lucchese R R, Bozek J D, Das A and Poliakoff E D 2007 *J. Chem. Phys.* **126** 244309
[32] Huber K P and Herzberg G 1979 *Molecular Spectra and Molecular Structure IV. Constant of Diatomic Molecules* (New York: Van Nostrand-Reinhold)
[33] Dunning Jr T H 1989 *J. Chem. Phys.* **90** 1007
[34] Kendall R A, Dunning T H Jr and Harrison R J 1992 *J. Chem. Phys.* **96** 6796
[35] Liu X-J, Lucchese R R, Grum-Grzhimailo A N, Morishita Y, Saito N, Prümper G and Ueda K 2007 *J. Phys. B: At. Mol. Opt. Phys.* **40** 485
[36] Lucchese R R, Montuoro R, Grum-Grzhimailo A N, Liu X-J, Prümper G, Morishita Y, Saito N and Ueda K 2007 *J. Electron. Spectrosc. Relat. Phenom.* **155** 95